Improving the performances of current optical interferometers & future designs
Proceedings of Haute Provence Observatory Colloquium (23-27 September 2013)
Edited by L. Arnold, H. Le Coroller & J. Surdej

Discrete beam combiners: 3D photonics for future interferometers

S. Minardi, A. Saviauk, F. Dreisow, S. Nolte, & T. Pertsch

Institute of Applied Physics, Abbe Center of Photonics,
Friedrich-Schiller-Universität Jena,
Max-Wien-Platz 1,07743 Jena, Germany

Abstract. We present the results of an experimental research aiming at investigating the potential of three-dimensional (3D) photonics for astronomical interferometry. We found that a simple two dimensional array of evanescently coupled waveguides (the so called Discrete Beam Combiner - DBC) can be used to retrieve the mutual coherence properties of light collected by three telescopes with a precision comparable to state-of-the-art interferometric beam combiners. On the basis of these results, we envisage the future use of DBCs in optical/IR interferometry, with particular attention to large arrays of telescopes.

1. Introduction

Photonics and, in particular, micro-optical components such as optical fibers and waveguides have started to play a more and more important role in optical/IR astronomical interferometry. Nearly two decades ago it was recognized how optical fibers could be used to perform effective spatial filtering and beam combination of telescopes (Coudé Du Foresto et al. 1996). The instrument FLUOR demonstrated unprecedented accuracy in the measurement of stellar visibilities (Coudé Du Foresto et al. 1998).

It was soon afterwards these pioneering experiments that Kern et al. (1996) proposed the use of planar integrated optical components (2D photonics) to miniaturize even further the optical setup for interferometric beam combination and enhance its thermo-mechanical stability. In the last decade, this proposal lead to the development and on-sky test of several prototypes designed to combine 2 (Berger et al. 2001), 3 (Berger et al. 2003) and 4 (Le Bouquin et al. 2011) telescopes simultaneously. The integrated devices allowed a considerable reduction of the size and maintenance tasks (such as alignment) of the interferometric instruments, while delivering first class scientific results. The main limitation of the planar integrated optics approach is that it is difficult to scale up the devices to allow the combination of a higher number of telescopes and baselines, as would be desirable for interferometric imaging applications. Integrated 8 telescope combiners were proposed but not yet realized (Berger et al. 2000). The difficulty in scaling up planar photonic beam combiners raises from the management of the increasing number of waveguide cross-overs required to distribute the light from the telescopes across the integrated optical chip.

In this context, recent technological advances have opened the perspective to manufacture fully three-dimensional (3D) photonic components, which in principle could solve the problem of scalability of planar integrated beam combiners. The technological platform of 3D photonics is based on the direct writing of transparent materials with tightly focused ultrashort (< 100 fs) laser pulses. Under irradiation of high intensity laser pulses a plasma is formed which develops in defects or a reconfiguration of the local material structure upon recombination. These structural modifications manifest themselves as local variations of the refractive index, which can be positive or negative depending on the type of irradiated material. By scanning the laser beam focus inside the material with a 3-axes positioning system, it is possible to inscribe complex refractive index structures in 3D.

Three dimensional photonic components have been considered very recently for astronomical interferometry as well (Rodenas et al. 2012, Jovanovic et al 2012, Minardi et al. 2012). Rodeans et al. 2012 used curved waveguides and Y-junctions written in chalcogenide glasses to combine three channels simultaneously. While representing the first experimental testbed of 3D photonics for multiple telescope combination, the work also showed the potential of direct laser writing to manufacture waveguides for mid-infared in non-standard glasses. The first 3D component to be tested on-sky was the Dragonfly photonic chip, where waveguides are used to remap 4 pupil apertures into a non redundant linear array of point-like sources for free-space multi-axial beam combination. The potential of pupil remapping techniques resides in the possibility to retrieve high-dynamical range images from seeing limited instruments and with a resolution close to the diffraction limit (Perrin et al. 2006). Finally, in Minardi et al. 2012 laboratory experiments showed that the design of a beam combiner can be radically simplified down to a two-dimensional regular array of coupled waveguides (the discrete beam combiner, DBC) (Minardi & Pertsch 2010). In all three cases, crossovers between waveguides were avoided thanks to the availability of a third dimension.

Here we present the results of an experimental research aiming at investigating the potential of the DBC and in general 3D photonics for astronomical interferometry. We have manufactured several DBC units for the combination of three beams and tested them in the laboratory with monochromatic (Minardi et al. 2012) and polychromatic light (Saviauk et al. 2013). We found that DBCs can measure visibility amplitudes and closure phases over a 50nm-broad visible band with a precision comparable to state-of-the-art interferometric beam combiners. Considering the successful laboratory demonstration of the concept, we will discuss perspectives for the application of DBCs to optical/IR interferometry, with particular attention to large arrays of telescopes.

2. Operation principle of a discrete beam combiner

According to the DBC method, to combine N telescopes a regular two dimensional square array of at least N x N evanescently coupled waveguides is used (see Figure 1). The light from the telescopes is injected into selected waveguides of the array. Due to evanescent coupling, light propagating in one waveguide will leak to neighboring waveguides. At a given length of the sample, the N input fields will interfere inside the waveguides with variable amplitude and phase depending on the observed waveguide and length of the sample. As a result, it is possible to retrieve the mutual coherence properties of every possible pair of telescopes from a measurement of the power carried by each waveguide.

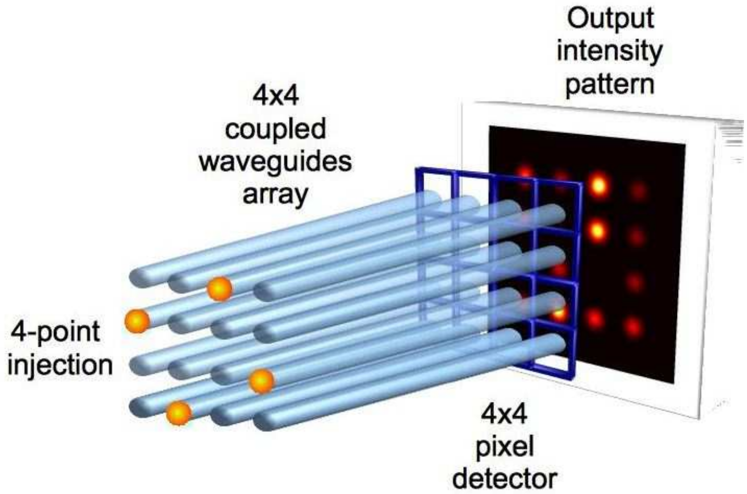

Figure 1.: *Conceptual design of the DBC. Light injected in selected sites of the waveguide array (highlighted in the drawing) is combined within the waveguides thanks to evanescent coupling. The discrete interference pattern is recorded then by an array of detectors matched to the waveguides. This pattern can be related to the mutual coherences of the input fields (see text for details).*

More specifically, the efficient combination of the fields $A_{\rm k}$ from N telescopes uses an array of $(N+1)\times(N+1)$ waveguides (Minardi 2012). The $(N+1)^2$ output intensities $I_{\rm n}$ of the waveguide modes at the end of the sample are thus related to the complex visibilities $\Gamma_{\rm jk} = \Gamma^*_{\rm kj} =< A_{\rm j}A^*_{\rm k} >$ by a real valued, $(N+1)^2 \times N^2$ elements matrix $\{\alpha\}$ (Minardi 2012):

$$I_{\rm n} = \sum_{\rm k=1}^{N^2} \alpha_{\rm n,k} J_{\rm k}. \tag{1}$$

Here the complex visibilities enter the equation in the form of their quadratures $J_{\rm k}$, that is the value of the field autocorreleation function (intensities: $\Gamma_{\rm ii}$) and the real and imaginary components of all possible complex visibilities. The matrix $\{\alpha\}$ is then nothing else that a form of the Visibility to Pixel Matrix (V2PM), usually employed to extract coherence information from multi-axial beam combiners (Tatulli et al. 2007). In terms of the quadratures of the complex visibilities, the commonly measured normalized fringe visibilities are defined as:

$$V_{\rm ij} = \sqrt{\frac{(\Re\Gamma_{\rm ij})^2 + (\Im\Gamma_{\rm ij})^2}{\Gamma_{\rm ii}\Gamma_{\rm jj}}} \quad {\rm i} \neq {\rm j}. \tag{2}$$

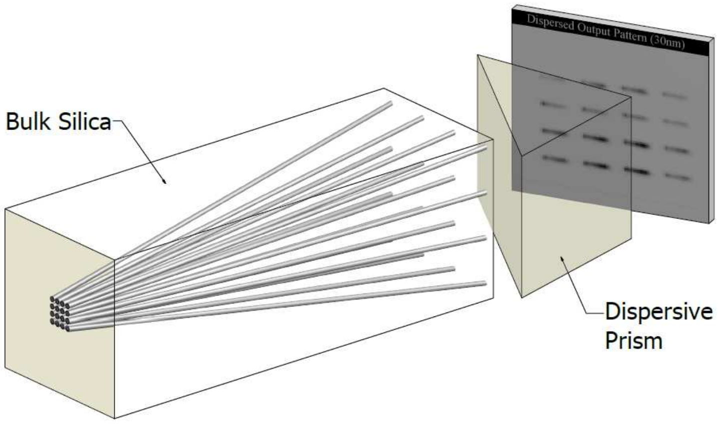

Figure 2.: *Conceptual sketch of a DBC sample for polychromatic operation. The beam combination takes place at the beginning of the tapered array of waveguides, where the inter-waveguide coupling is large. As the light propagates further in the sample, the coupling becomes negligible and the interference pattern of the modes becomes frozen. The waveguides are brought far apart so that an imaging spectrograph (here represented by a prism) can project the spectra of the light carried by the individual waveguides in the gap between them.*

The corresponding phases $\phi_{\rm ij}$ are defined as:

$$\phi_{\rm ij} = \tan^{-1} \frac{\Im \Gamma_{\rm ij}}{\Re \Gamma_{\rm ij}} \tag{3}$$

The unknowns $J_{\rm k}$ are retrieved from the individual interference measurements $I_{\rm n}$ by estimating the pseudo-inverse of the matrix α. The matrix elements can be calculated from first principles (Minardi & Pertsch 2010, Minardi 2012), or determined experimentally (Saviauk et al. 2013) by a column-wise calibration procedure, as used by Lacour et al. 2008 for planar photonic beam combiners. The best input configuration, array geometry and length is associated to the matrix $\{\alpha\}$ featuring the smallest condition number, meaning that the error propagation from the measured $I_{\rm n}$ to the complex visibilities $J_{\rm k}$ is minimal.

Notice that the coupling between neighboring waveguides is usually very sensitive to the wavelength of light and for this reason we expect the DBC method to work for relatively narrow bandpasses. To increase the operation bandwidth of the component, we designed and tested the tapered DBC component illustrated in Fig. 2. At the beginning of the sample, strong inter-waveguide coupling allows the DBC to operate. The coupling decreases as the waveguides are driven apart, so that the interference pattern formed at the beginning is frozen in the waveguides. At the end of the sample the separation between waveguides is large enough so that it is possible, by means of an imaging spectrograph, to project low resolution frequency spectra of the light coupled in each individual waveguide in the gaps between them. By analyzing the DBC pattern of light at each individual color, it is possible to determine the coherence properties of the combined light wavelength by wavelength.

3. Laboratory performance of the discrete beam combiner

We present now the laboratory characterization of a DBC prototype manufactured to combine simultaneously three telescopes and operate between the wavelengths of 640 nm and 690 nm. This wavelength range was dictated by the available white light source and optical equipment of our laboratory, but are representative of what could be achieved at other wavelengths, for instance in the near- or mid-infrared. The setup used to test the DBC is illustrated in Figure 3. The beams of the three telescopes were simulated by the three channels of the modified Mach-Zehnder interferometer of Fig. 3. The complex visibilities arising from the interference of pairs of beams chosen from the three channels represent the visibilities of a baseline (baseline1=Beam1-Beam2, baseline2=Beam1-Beam3, baseline3=Beam2-Beam3). The three beams are focused on the input waveguides of the DBC component, as illustrated in the inset picture. Finally, the output light pattern is dispersed in an imaging spectrograph and recorded on a CCD camera.

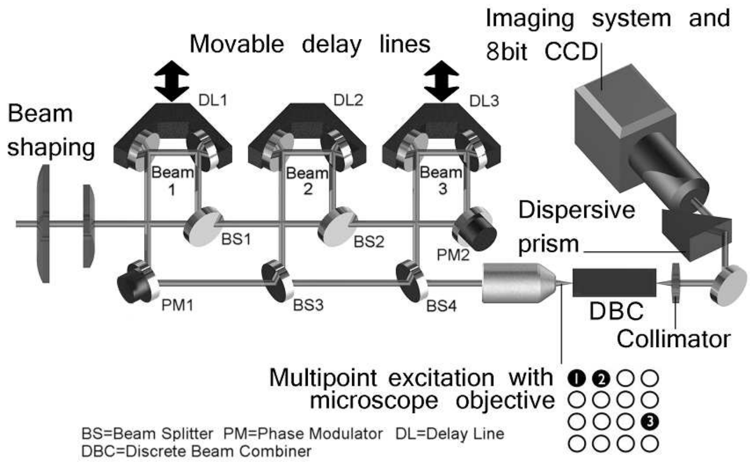

Figure 3.: *The setup of the DBC test-bench. In the inset: the injection points of the light in the DBC component.*

We have characterized the combination performance of the DBC method with polychromatic light. To this end, we have tested the capability to retrieve the photometry, the normalized visibility and the phase of the fringes across the chosen spectral range. Figure 4 addresses the photometric performance and shows the normalized intensities of three input beams as a function of wavelength. The average values of the beam intensities J_1, J_2 and J_3 and their standard deviation were measured. Data show that the mean values have a slightly non-constant trend which is due to the transmission spectrum of the beam splitters in the

Mach-Zehnder interferometer, as proved by the dashed lines representing the model of the beam splitters.

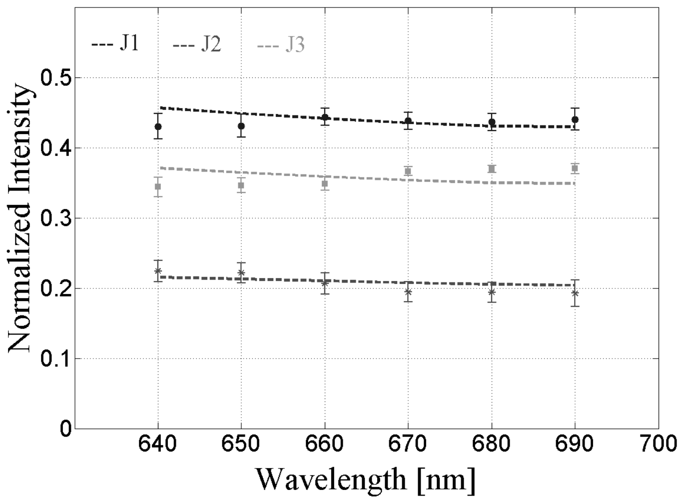

Figure 4.: *The retrieved photometry from DBC measurements at different wavelengths. The slight trend in the photometry is attributed to the transmission spectrum of the beam splitters of the test bench. Lines: fit model of the test bench.*

We next verified that our system can deliver high visibilities throughout the analyzed spectral range. We set the optical path difference between the three input beams to 0 for light at $\lambda_c = 660$ nm. The optical path of the beams 1 and 3 was then modulated independently with a $\pm 6\mu$m stroke with rates of 5.2 μm/s. The recorded the DBC output was used to retrieve by means of Eq. 2 a time series of the normalized visibilities. The average values of the visibility and its standard deviation are plot as a function of the wavelength in Fig. 4 for the three different baselines of our interferometric setup. The visibility of the three baselines is constant within the error bars and its average value over all baselines and all wavelengths is 0.88 ± 0.06, allowing a raw visibility dynamics of about 15. Part of the residual variation of the visibilities over wavelength may be attributed to the chromatic dispersion of the beam splitters.

With the same data we tested also the spectral uniformity of the DBC method in retrieving optical path difference (OPD) data. The measured OPD variation between beams 2 and 3 was 24.6 μm and was constant within 70 nm across the investigated wavelength range. Another crucial parameter for astronomical imaging is the stability of the closure phase. In our case the closure phase is defined as $\Phi_C = \Phi_{12} + \Phi_{32} - \Phi_{13}$. We have measured the standard deviation of the closure phase for different wavelengths as illustrated in Fig. 9. We have obtained a stability better than $\lambda/36$ over the whole bandwidth of 50 nm with a minimum value of $\lambda/58$ at a wavelength of 650 nm (11 nm optical path difference). Notice that planar beam combiners for astronomical interferometry were reported to have a closure phase stability of $\lambda/144$ at a wavelength of 1550

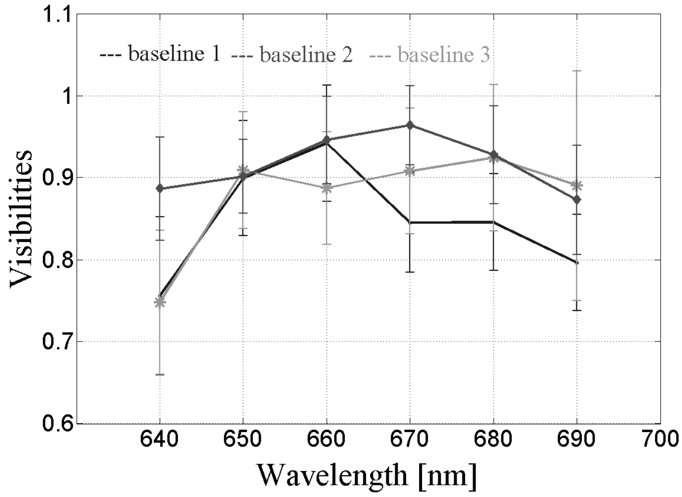

Figure 5.: *The retrieved visibility modulus from DBC measurements at different wavelengths and different baselines.*

nm (Benisty et al. 2009). This corresponds to an optical path difference of 11 nm, as reported in our experiments at the wavelength of 650 nm.

4. Applications of DBC and the future of optical/IR interferometers

Applications of DBCs can be found in laser metrology and astronomical interferometry. In its simpler form (straight waveguide array), the DBC can already be used to perform high precision laser metrology simultaneously over many beams, as required for instance for the delay lines of a multi-telescope interferometer. In particular, the possibility to measure the optical path differences between the injected beams would be an advantage for interferometers operating in dual-star mode (Lane & Colavita 2003, Sahlmann et al. 2013), where the precise knowledge of the differential position of delay lines is required to perform astrometric measurements. In the near future it will be possible to extend the dual-star mode to more baselines, so that simultaneous monitoring of several differential delay lines will be required (Gillessen et al. 2012).

Another application for DBC in future interferometers could be the monitoring of optical path differences in networks of optical fibers (Minardi et al. 2009, Spaleniak et al. 2010). Indeed a long term goal for interferometry is the achievement of fibered links between telescopes, a scheme which would allow the realization at sustainable costs of kilometric baseline interferometers (Mariotti et al. 1996, OHANA) The guided wave optics interface of DBC makes them natural candidates to be integrated in fibered optical networks.

Beside these applications, imaging spectro-interferometry is the field where we expect the DBC to have a major impact. Two are the advantages that the application of DBC can bring to this field of astronomy, namely 1) enhanced

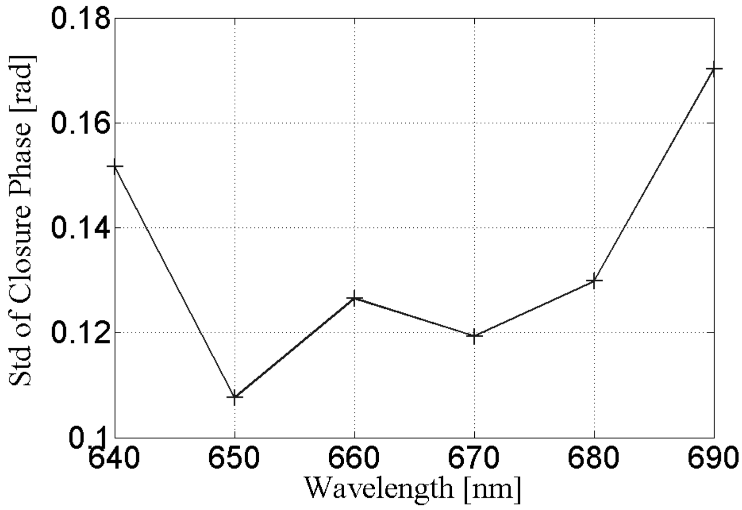

Figure 6.: *The standard deviation of the measurement of the closure phase from DBC data.*

sensitivity and 2) possibility to combine very large arrays of telescopes. As compared to multi-axial combiners (Monnier et al. 2004, Jovanovic et al. 2012), the advantage of the DBC is potentially that of spreading light on a minimal number of pixels per wavelength. Indeed each of the output waveguides could be imaged onto a single pixel of an arrayed detector resulting in $(N+1)^2$ pixels per wavelength required to retrieve the whole coherence portrait of the sampled optical fields. This is much smaller than the number of pixels employed typically in multiaxial combiners (compare e.g. Jovanovic et al. 2012), thus resulting in enhanced sensitivity. There is a slight sensitivity advantage also compared to ABCD integrated beam combiners, where the number of pixels per wavelength scales as $2N(N-1)$ (4 times the number of baselines). DBC combining more than 4 telescopes should be more sensitive than the ABCD combiners, even though slight (for 10 telescopes the advantage is quantified in about 0.5 magnitudes).

The second advantage as compared to current integrated combiners is that DBC could be easily scalable to large number of telescopes while retaining the simplicity of their structure. Numerical simulations have tested the capability of the DBC to combine 6 telescopes (Minardi 2012), but there are no fundamental reasons to prevent from using the scheme for the combination of larger arrays. The difficulty is mainly related to the computational cost of finding the input configuration of the DBC, allowing for a reasonable stability of the coherence reconstruction method (condition number of the V2PM matrix below ≈ 15).

It is certainly the simplicity of the design and the flexibility of the manufacturing method which makes DBC particularly attractive for astronomical applications. We note that this is particularly true for non-telecom wavelengths such as required for astronomy. Indeed, conventional photonic manufacturing technologies cannot be applied for instance for materials suitable for mid-infrared (such as chalcogenide glasses). Direct laser writing can be used to manufacture

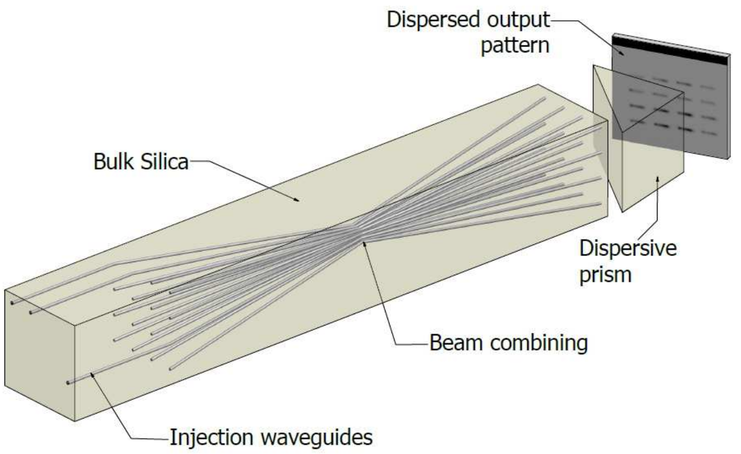

Figure 7.: *Conceptual setup of a component integrating an input modal filtering and beam combination.*

waveguides in a wide range of materials and the DBC scheme offers the simplest 3D photonic circuit that allows the measurement of coherences.

Looking into the future, we may think of a 3D photonic chip integrating several functionalities. An example is given in Figure 7. The chip includes a mode filtering section and a DBC. It could be foreseen that the final dispersive element could also be integrated by connecting the output waveguides through fibers to Arrayed Waveguide Gratings (Cvetojevic et al. 2009) or even more integrated solutions such as the photonic crystal superprism (Momeni et al. 2009).

5. Conclusions

We have explored the potential of 3D photonics for applications to astronomical interferometry and found that the design of photonic beam combiners can be greatly simplified by the addition of the third dimension. We investigated in particular the beam combination properties of regular arrays of evanescently coupled waveguides (DBC), showing that they can deliver full interferometric information with a quality comparable to existing beam combiners. Advantage of the DBC scheme is the simplified design and scalability to the combination of large numbers of telescopes (6 or more). The applicability of the DBC can range from metrology to science data collection in multi-telescope interferometers. Future developments of the DBC concept include exploring exotic geometries of the array of waveguides to make the beam combination even more effective.

References

Benisty, M., et al., 2009, A&A 498, 601

Berger, J.-P., et al. 2000, Proc. SPIE 4006, 986

Berger, J.-P., et al., 2001, A&A 376, L31

Berger, J.-P., et al., 2003, Proc. SPIE 4838, 1099

Coudé Du Foresto, V., et al. 1996 in *Astrofib: Integrated Optics for Astronomical Interferometry*, p. 115

Coudé Du Foresto, V., et al. 1998, Proc. SPIE 3350, 856

Cvetojevic, N., et al., 2009, Opt. Exp. 17, 18643

Gillessen, S., et al., 2012, Proc. SPIE, 8445, 84451O

Itoh, K., et al., 2006, MRS Bulletin 31, 620

Jovanovic, N., et al., 2012, MNRAS 427, 806

Kern, P. , et al., 1996, in *Astrofib: integrated optics for astronomical interferometry*, p. 195

Lacour, S., et al., 2008, Proc. SPIE 7013, 701316

Lane, B. F., & Colavita, M. M., 2003 AJ 125, 1623

Le Bouquin, J.B., et al., 2011, A&A 535, A67

Mariotti, J.M., et al. 1996, A&A 116, 381

Minardi, S., et al., 2009, Astron. Nachr. 330, 518

Minardi, S., & Pertsch, T., 2010, Opt. Lett. 35, 3009

Minardi, S., 2012, MNRAS 422, 2556

Minardi, S., et al., 2012, Opt. Lett. 37, 3030

Momeni, B., et al., 2009, Opt. Comm. 282, 3168

Monnier, J. D., et al., 2004, Proc. SPIE 5491, 1370

Perrin, G., et al., 2006, MNRAS 373, 747

Sahlmann, J., et al., 2013, A&A 551, A52

Saviauk, A., et al., 2013, Appl. Opt. 52, 4556

Spaleniak, I. et al., 2010, Proc. SPIE 7734, 77343Y

Tatulli, E., et al., 2007, A&A 464, 29